IEEE Open Journal of Nanotechnology

Received 3 November 2020; revised 1 December 2020; accepted 4 December 2020. Date of publication 14 December 2020; date of current version 4 January 2021. The review of this article was arranged by Associate Editor Lixin Dong.

Digital Object Identifier 10.1109/OJNANO.2020.3044352

Detection of Transferrin Receptor CD71 on a Shear Horizontal Surface Acoustic Wave Biosensor

XUE-CHANG LO [1], MING-TSANG LEE [2], AND DA-JENG YAO [3] (Senior Member, IEEE)

[1]Department of Engineering and System Science, National Tsing Hua University, Hsinchu City 30013, Taiwan
[2]Department of Power Mechanical Engineering, National Tsing Hua University, Hsinchu City 30013, Taiwan
[3]Institute of Nano Engineering and Micro Systems (NEMS) in National Tsing Hua University, Hsinchu City 30013, Taiwan

CORRESPONDING AUTHOR: DA-JENG YAO (e-mail: djyao@mx.nthu.edu.tw)

This work was supported by the Taiwan Ministry of Science and Technology under Grants MOST 108-2321-B-866-001 and MOST 107-2321-B-886-002.

ABSTRACT A semi-empirical model was applied to estimate the frequency shift of a shear-horizontal surface-acoustic-wave (SH-SAW) biosensor for detecting a disease-related biomarker antigen transferrin receptor (CD71) in the sample. In the simulation to investigate its sensitivity, a shift of the SH-SAW resonant frequency occurred by applying an incremental surface mass density change on the surface. The semi-empirical model was proposed and developed by using the experimental and numerical results to relate the concentration of the biomarker to the frequency shift. Results indicated that the thickness of the SiO2 guiding layer affects the sensitivity of SH-SAW sensing, and the dependence is non-monotonically. The SH-SAW sensor was used for specific detection of biotin at a varied concentration. With the concentration of the targeted antigen in the range 0.4 ~4.2 μg/mL, a typical exponential relation was found between the quantitative target and the frequency shift. Measurement results showed that the mass-loading effect of the antibody-antigen has a reliable response with a sensitivity of 0.94 kHz/(μg/mL). Effects of the sample flow rate on the antigen- antibody interaction and thus the frequency shift of the SH-SAW sensor were also evaluated. It is demonstrated that the proposed model provides a useful approach to analyze effectively the frequency shift dependence on the concentration and the flow rates of sensed molecules in a flow-type SH-SAW sensor.

INDEX TERMS Shear-horizontal surface-acoustic-wave (SH-SAW) biosensors, transferrin receptor, frequency shift, CD71.

I. INTRODUCTION

Surface acoustic-wave (SAW) sensors have been widely applied in biochemical fields such as biomarker detection [1]. In these devices, a transmitting interdigital transducer (IDT) generates a SAW on a piezoelectric substrate, which propagates through a delay line to the receiving IDT [2]. The SAW properties such as frequency, phase and velocity, may change corresponding to the mass loading and the perturbation on the functionalized sensing film, therefore makes the sensor able to detect specific biomarker [3]. On the other hand, a shear-horizontal wave is obtained when a wave-guiding layer of appropriate thickness and piezoelectric substrate properties is determined. The shear-horizontal fluctuation analysis is suitable for an interface between a wave- guiding layer and an external solid or liquid medium being measured. Therefore, the shear-horizontal SAW (SH-SAW) device especially has benefits in biological applications in liquids [4]. In fact SH-SAW device have been successfully applied to detect bacteria, the DNA hybrid reaction and cancer cells [5]–[7].

The sensitivity of a SH-SAW device under mass loading is determined by the acoustic velocity and thickness of the wave-guiding layer [8]–[10]. The optimal thickness of the guiding layer depends on its mechanical properties, which can be determined theoretically or experimentally [11], [12]. For example, finite-element method (FEM) have effectively been used to analyze the frequency response on applying a voltage to propagate at the surface of the device [13]–[15]. The results indicate that the sensitivity of the device could be

predicted reasonably accurate with varied guiding layers and samples. The mass sensitivity and other electromechanical properties as well as the optimization of SH-SAW sensors have been also demonstrated by using FEM analysis, and were validated by experimental results [16]. Specifically, in a previous study, a SH-SAW biosensor was used to capture the antibody of epidermal growth factors (EGF) reliably and with great sensitivity. [17]. A semi-empirical model for the relation of frequency shift and the concentration of the specific biomarker was proposed for rapid estimation based on the numerical simulation. The model is useful to estimate accurately the frequency shift of the SH-SAW sensor while diminishing the complication of the analysis of mass transport on the sensing film.

An SH-SAW sensor can be functionalized by applying self-assembled film with streptavidin molecules modified on a sensing surface to bind a specific biotinylated antibody of Transferrin receptor, for example, CD71. The streptavidin-biotin system has been intensively investigated and is widely applied in biochemical fields utilizing the high affinity between streptavidin and biotin in antigen-antibody interactions[18], [19]. The signal can be amplified under a multilevel combination process in immunoassay research [20]. Transferrin is the main iron-transfer protein in plasma. It imports the iron from transferrin into cells on interacting with a particular protein membrane receptor, CD71 [21]. CD71 expression is altered to become a likely predictive feature of multiple cancer cells or disease signs [22]–[24]. A determination of the quantity of CD71 has hence significant benefits for disease diagnostics and clinical applications. Standard assays of CD71 cells are currently based on immunological methods such as immunoradiometric assays (IRMA) [25], enzyme-linked immunosorbent assays (ELISA) [26] and immunonephelometry [27]. These methods are typically time-consuming, complicated and expensive. We hence investigated the feasibility of applying a SH-SAW sensor to detect CD71 at various concentrations in biofluids.

With the progress and development of immunological technology, the rate of the antigen-antibody reaction which is involved in a clinical diagnosis or a specific treatment is becoming increasingly important. There are many factors affecting the reaction rate and thus the sensitivity of the sensor, such as concentration, temperature, pressure and the reactant itself, which leads to a complicated mass-transport analysis. Several studies of SH-SAW devices have investigated optimizing the sensitivity by a determination of an optimal thickness of a guiding layer or increasing the microstructure designed [28]–[30]. In this work, we analyzed a SH-SAW sensor to investigate factors influence the mass sensitivity using numerical simulation. Representative devices were subsequently fabricated to perform experiments for validating the simulation results. On the basis of a previous research [17], a semi-empirical model was proposed to correlate the concentration of biomolecules with the frequency shift of the SH-SAW sensor.

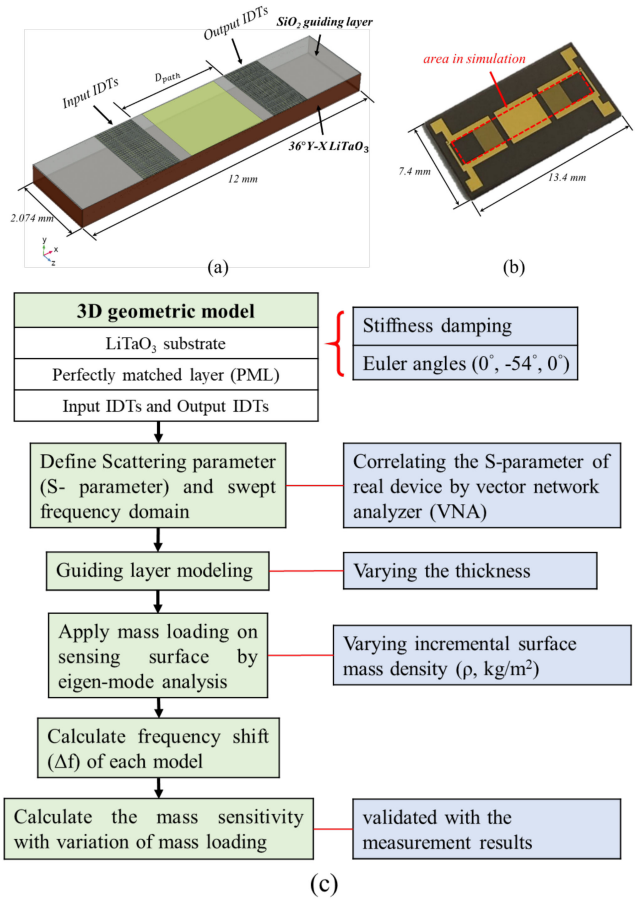

FIGURE 1. (a) Three-dimensional model of the device used in numerical simulation. (b) Fabricated SH-SAW chip without SiO2 layer. The selected area for simulation is marked with a red rectangle. (c) Simulation procedure.

II. MATERIALS AND METHODS

A. SIMULATION METHOD

To investigate the sensitivity and the shear horizontal wave characteristics, a FEM analysis was performed (COMSOL Multiphysics) based on a 3D piezoelectric-effect model. The constitutive equations were solved to relate the applied electric potential and the induced mechanical displacement. Details of the theory for piezoelectric analysis are available in [31].

Fig. 1 shows the geometry of the device simulated in this work. The basic geometric definition of the SH-SAW is similar as for a previous approach [17] which composed of a delay line SH-SAW device with a 36° Y-X LiTaO3 substrate and a SiO2 guiding layer deposited on the sensing surface. Detailed parameters of the IDTs are listed in Table 1. The characteristic resonance wavelength (λc) corresponds to a fundamental oscillation frequency from 120.6 MHz to 123.8 MHz. The sensing area was defined in the middle of these two sets of IDT. The simulation structure has a width of 2.074 mm (61 λc) in the z-direction. The delay line between the input and the output IDTs has a distance 4420 μm. The substrate thickness

TABLE 1. IDT Design Parameters

Parameters	Settings
Designed resonance wavelength (λ_c)	34 μm
SH-SAW velocity	4100–4212 m/s
Number of fingers	50 pairs
Finger width	8.5 μm
Thickness of electrodes	220 nm

is 500 μm, while the thickness of the guiding layer was varied to investigate its effect.

For generating a SAW, electric signal 5 V was applied to the odd electrode fingers of the input IDT while the even fingers were grounded. The output signals were acquired at the output IDT. A PML of thickness 6 λc was set from the boundaries of the device to minimize the reflection of the wave from the boundaries of the device [32]. Euler angles (0°, −54°, 0°) was set to define the orientation of the substrate with respect to the global coordinate in the simulation. Based on preliminary tests of the grid convergence, the mesh consisting of 90, 772 elements was adopted of further simulation.

A dual-port circuit model was solved in the frequency domain. With voltage signals applied to the terminals, the extracted current is present as admittance. The relation between admittance (Y-parameter) and scattering parameter (S-parameter) establishes an equivalent circuit model [33]. To obtain the mass sensitivity of the SH-SAW device, the frequency shift (Δf) with adding an incremental surface mass density (ρ, kg/m2) on the SiO2 layer was calculated to present a mass loading of the device with an Eigen-mode analysis. For the proposed semi-empirical model [17], the incremental surface mass density with respect to the biomolecule concentration $\Delta\rho$ for a specific SH-SAW sensor corresponding to the concentration of a target molecule is determined by applying the relation:

$$\Delta\rho = k_1 e^{(-k_2/c0)}/m_{sub} \tag{1}$$

in which c0 is the molecule concentration of the measuring sample, *m*sub is the mass per area of the substrate, *k*1 and *k*2 are empirical coefficients to be evaluated by comparing the simulation and experimental results. With this model, the dependence of Δf on $\Delta\rho$ is readily converted to the dependence of Δf on c0 after the corresponding empirical coefficients are determined.

B. FABRICATION OF SH-SAW SENSORS

The SH-SAW chip with a delay-line structure was fabricated with a typical MEMS method, including lithography development, e-beam evaporator and lift-off on 36° Y-X black $LiTaO_3$ of thickness 0.5 mm. An Au/Cr metal layer (200/20 nm) was deposited with an e-beam evaporator including the sensing area and IDT. Thicknesses 0.5, 0.8 and 1.4 μm of a SiO_2 guiding layer were then deposited on the delay lines and IDT with plasma-enhanced chemical vapor deposition.

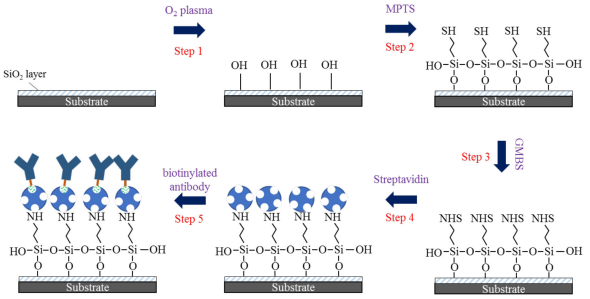

FIGURE 2. Processing steps of biochemical surface modification of the SiO2 layer.

C. SURFACE FUNCTIONALIZATION

To capture specifically and selectively the target protein, the surface of the sensing section was functionalized as illustrated in Fig. 2. The chip was first treated with O2 plasma to enrich the surface with –OH bonds [34]. The sensing surface was then silanized with immersing in a solution of 3-mercaptopropyl trimethoxysilane (MPTS, 4%, Sigma, 175617) in ethanol (99.5%) for 2 h. The surface with hydroxyl groups underwent a condensation with the methoxy groups of MPTS and was covered with sulfydryl (–SH) [35]. After rinsing with pure ethanol and drying with N_2, a cross-linker of 4-maleimidobutyric acid N-hydroxysuccinimide ester (GMBS, 200 ug/mL, Sigma, 63175) in ethanol was connected with the sulfydryl for covalent bonding of the streptavidin (200 μg/mL, Biosynth Carbosynth, 9013-20-1) diluted in phosphate- buffered saline (pH 7.4, PBS) and immersed for 5 h [36], followed by PBS rinsing and nitrogen blow-drying. To activate the sensing area, biotinylated antibodies of Transferrin receptor CD71 (100 μg/mL, Sigma, SAB4700517) were assembled on the sensing surface of the sensor device for 3 h [37].

D. SH-SAW SENSING SYSTEM

Fig. 3 shows the experiment setup. The fluid was pumped into the reaction cell with a microfluidic system (Fluigent MFCS-EZ) composed of a PMMA flow channel allowing biomolecules to flow on the sensing surface continuously and stably with air-tight. These devices were connected in a positive-feedback circuit, resulting in SAW oscillators for signal detection. A power supply (Keysight E3611A) provided the input voltage. A frequency counter (Keysight 53220A) was used to measure the frequency output from the readout electronics package. The instant frequency shift was recorded with a universal counter control and automation program (Keysight BenchVue). Other details for this dual-delay-line measurements could be found in reference [17].

III. RESULTS AND DISCUSSION

A. NUMERICAL ANALYSIS

The corresponding relation between the *S*-parameter and the *Y*-parameter can be determined with the *S*-parameters

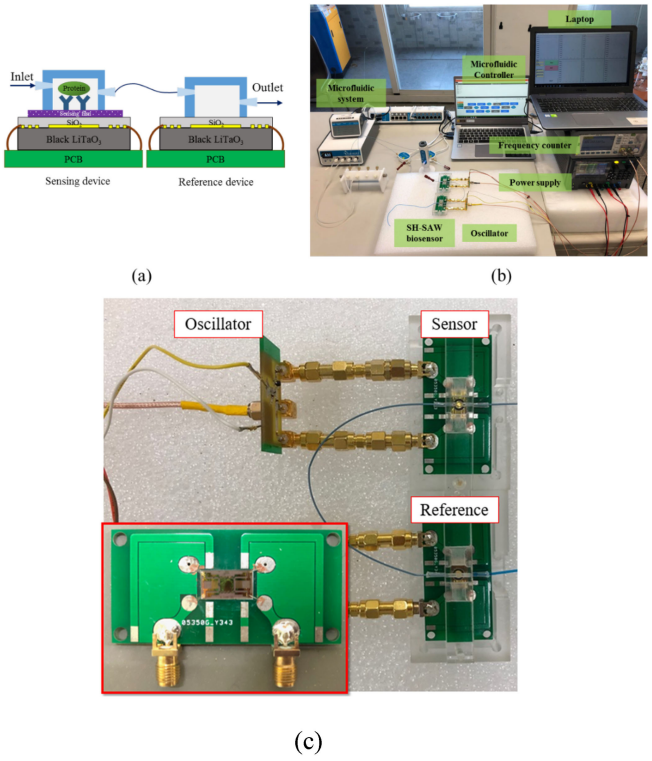

FIGURE 3. **(a) Configurations of the dual SH-SAW biosensors. (b) Experiment apparatus. (c) The dual SH-SAW biosensors and the circuitry board (the insert).**

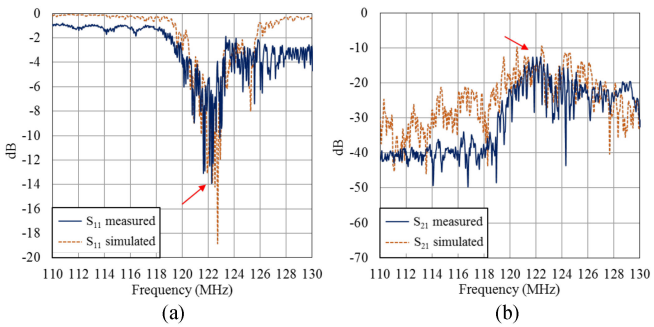

FIGURE 4. **Comparison of (a) *S*11 and (b) S_{21} between simulated and measured frequency responses in the range of major resonance frequencies. Arrows indicate the location of the center frequency.**

obtained from the simulation and experiments. In the experiment, the *S*-parameters in the SAW delay line were measured with a vector network analyzer (VNA). A comparison between the simulation results and experimental measurements illustrated in figure 4 shows a reasonably good agreement on the frequency spectrum. The simulation results of S_{11} show a pronounced resonance frequency (122.6 MHz) similar to the measured results (122.3 MHz) for the designed center resonance frequency. The typical insertion loss (IL) S_{21} of the fabricated SH-SAW devices was approximately −13 dB and demonstrated reasonably good agreement between the simulation and experimental results near the center frequency.

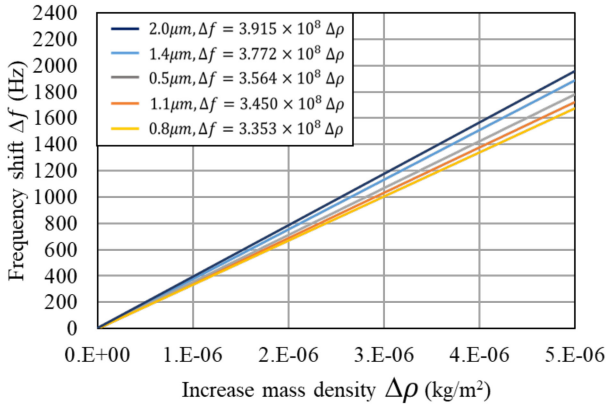

FIGURE 5. **Simulated results of frequency shift (Δ*f*) with respect to incremental surface mass density (Δ$_\rho$).**

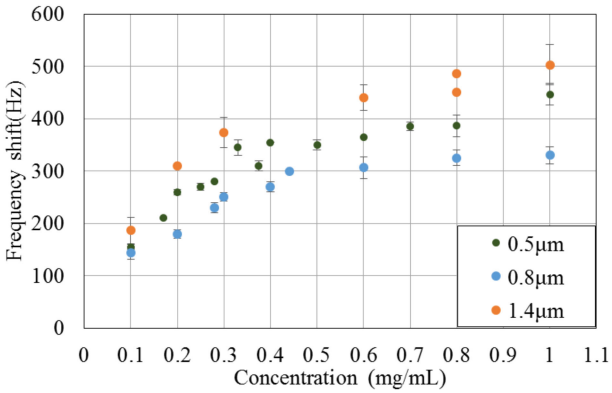

FIGURE 6. **Experimental results of frequency shift with varied concentration of biotin. Measured results are shown for thicknesses 0.5, 0.8 and 1.4 μm of the guiding layer; each data point represents an average of three measurements with standard deviation.**

The frequency shift changes with respect to the mass loading are evaluated to determine the mass sensitivity of the sensor. The incremental surface mass density (ρ, kg/m^2) of the sensing surface varied from 0 to 5×10^{-6} kg/m^2 was applied to investigate the corresponding frequency shift of SiO_2 with varied thickness. Numerical results of the Eigen-mode response sensitivity of device are shown in Fig. 5. The slope of each line represents the mass sensitivity of each thickness. The sensitivity of the device varies non-monotonically with respect to the thickness of the guiding layer. The coupled resonance of appropriate guiding layer thickness can improve the mass sensitive of the device [38], as was also illustrated from the results shown in Fig. 5.

B. RESPONSE FREQUENCY OF A SH-SAW BIOSENSOR WITH BIOTIN PROTEIN

In the experiment, biotin protein at varied concentration was used to detect the response frequency with guiding layers of three thicknesses to evaluate the mass sensitivity. As Fig. 6 shows, the stabilized frequency shift increases with the concentration of biotin before saturated. The dependence differed for thicknesses 0.5, 0.8 and 1.4 μm of the guiding layer. Noted

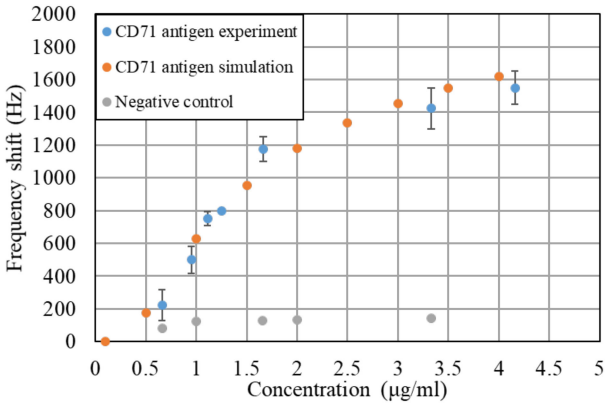

FIGURE 7. Experimental and simulation results of CD71 protein for the frequency shift.

that the experiments for guiding layer thicknesses of 0.5, 0.8 and 1.4 μm were repeated more than fifteen times to ensure the repeatability of the data.

In all three cases the generated acoustic energy is efficiently transmitted with the guiding layer to the sensing surface, markedly increasing the device sensitivity [38], [39]. The measured results showed that the streptavidin-biotin reaction has a reliable response due to mass-loading effects. It is obvious that the mass sensitivity does not change monotonically with the thickness of the guiding layer. As predicted by the numerical simulation results shown in Fig. 5, the frequency shift is highest for the thickness of 1.4 μm and lowest for the thickness of 0.8 μm at a specific protein concentration. It is thus evident that the current numerical simulation is consistent with the experiments in terms of the characteristics of sensitivity, which enables the optimization of the sensor design by applying the simulation.

C. RESPONSE FREQUENCY OF A SH-SAW BIOSENSOR WITH CD71 PROTEIN

Before the interaction of the antigen and the antibody, the biotinylated antibody of CD71 was immobilized on the sensing film, which consisted of modified streptavidin molecules. The SH-SAW sensor with a guiding layer of thickness 0.5 μm SiO_2 was selected in this configuration. The flow rate of the sample containing CD71 protein is 2 μL/min. The frequency shift of the SH-SAW sensors varied with concentration of the CD71 antigen as shown in Fig. 7. The experiment for CD71 antigen measurement was repeated nineteen times and the standard deviation is shown on the figure. A typical exponential relation was found between the concentration and the frequency shift of the SH-SAW sensor. The sensitivity level is found to be 0.97 kHz/(μg/mL) for a biomarker concentration less than 1.66 μg/mL. A negative control measurement was performed using IgG protein. The maximum frequency shift of the negative control was approximately 100 Hz, which might be due to a small amount of molecules sticking to the surface. The experimental results for the CD71 protein

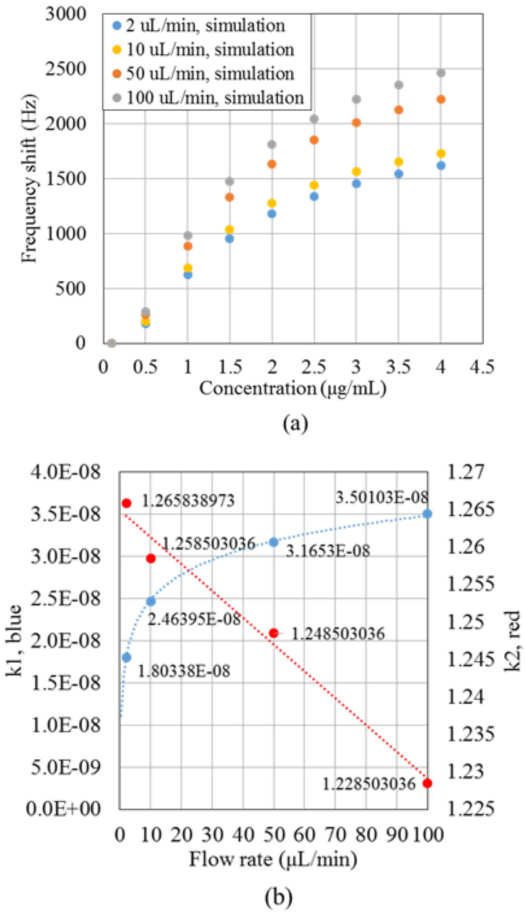

FIGURE 8. (a) Simulation results of CD71 protein for the frequency shift with varied flow rate (b) distribution between k_1 and k_2 at varied flow rate.

showed a reliable response of this immunosensor to the mass-loading effects of the antibody-antigen reaction. It should also be noted that at low concentration (~0.5 μg/mL) the frequency shift is approximately 200 Hz. The influence from the noise showing in the negative control should be carefully considered in this range.

D. SEMI-EMPIRICAL CORRELATION MODEL FOR A SH-SAW BIOSENSOR

The simulated frequency shift corresponding to an increased mass density of the sensing surface, as shown in Fig. 5, can be converted to the frequency shift on CD71 concentration using Equation (1) with using the experimental results shown in Fig. 7 to evaluate k_1 and k_2. Empirical coefficients are determined to be $k_1 = 1.803 \times 10^{-8}$, $k_2 = 1.265$ and the mass sensitivity is 3.565×10^8 Hzm^2/kg in the current configuration. The response frequency shift correlated with the antibody-antigen reaction was measured at flow rates of 2, 10, 50 and 100 μL/min of the CD71 protein, and the empirical coefficients were determined correspondingly. As shown in Fig. 8(a), the proposed semi-empirical model demonstrate that the frequency shift increases with increasing the flow rate. It is possible that the pressure from of the flow added

a virtual mass loading on the sensing surface with increasing flow rate which would affect the sensor response in addition to the antibody-antigen reaction. Another possibility is the affinities in the analyte binding for the immobilized antibody of a surface varied with the flow rate [40]. This effect might result in a significant increasing binding rate when the flow rate is increased.

From the results of k_1 and k_2 shown in Fig. 8(b), an exponential and a linear trend were found, respectively. It should be pointed out that once those empirical coefficients were evaluated, the response frequency shift of the CD71 protein corresponding to varied flow rates and concentrations can be quickly calculated. of the SH-SAW biosensor.

IV. CONCLUSION

This research presented numerical simulation and experiments to investigate the mass sensitivity of a SH-SAW sensor and its frequency shift, for the detection of cancer-related biomarker antigen CD71. The center frequency was found to be 122.6 MHz and 122.3 MHz from simulation and measurement, respectively. The mass sensitivity of the device with varying the guiding layer thickness was also investigated by analyzing the corresponding frequency shift. A reliable consistency was found between the simulation prediction and the experimental results. With the concentration of the targeted biomarker (CD71) varied from 0.66 to 4.16 μg/mL, a typical exponential relation was found between the concentration and the frequency shift of the SH-SAW sensor. The sensitivity level was found to be 974 Hz/(μg/mL) for a biomarker concentration less than 1.66 μg/mL. The experimental results showed a clear response of this immunosensor to the mass-loading effects of the antibody-antigen reaction. On the basis of the experimental and numerical results, a semi-empirical model was applied to determine the frequency shift corresponds to the concentration of the biomolecules. The empirical coefficients were further evaluated from correlating the experimental results at varied flow rate of the sample. The proposed model demonstrates a useful approach to analyze effectively the frequency shift dependence on the concentration of sensed molecules.

REFERENCES

[1] L. Du, C. Wu, Q. Liu, L. Huang, and P. Wang, "Recent advances in olfactory receptor-basedbiosensors," *Biosens. Bioelectron.*, vol. 42, pp. 570–580, 2013, doi: 10.1016/j.bios.2012.09.001.

[2] R. White and F. Voltmer, "Direct piezoelectric coupling to surface elastic waves," *Appl. Phys. Lett.*, vol. 7, no. 12, pp. 314–316, 1965.

[3] I. Voiculescu and A. N. Nordin, "Acoustic wave based MEMS devices for biosensing applications," *Biosens. Bioelectron.*, vol. 33, no. 1, pp. 1–9, 2012.

[4] M. Tom-Moy, R. L. Baer, D. Spira-Solomon, and T. P. Doherty, "Atrazine measurements using surface transverse wave devices," *Anal. Chem.*, vol. 67, no. 9, pp. 1510–1516, 1995.

[5] I. Borodina, B. Zaitsev, G. Burygin, and O. Guliy, "Sensor based on the slot acoustic wave for the non-contact analysis of the bacterial cells–Antibody binding in the conducting suspensions," *Sensors Actuators B: Chem.*, vol. 268, pp. 217–222, 2018, doi: org/10.1016/snb.2018.04.063.

[6] Y. Hur, J. Han, J. Seon, Y. E. Pak, and Y. Roh, "Development of an SH-SAW sensor for the detection of DNA hybridization," *Sensors Actuators A: Phys.*, vol. 120, no. 2, pp. 462–467, 2005.

[7] K. Chang *et al.*, "Label-free and high-sensitive detection of human breast cancer cells by aptamer-based leaky surface acoustic wave biosensor array," *Biosens. Bioelectron.*, vol. 60, pp. 318–324, 2014.

[8] G. Kovacs, G. Lubking, M. Vellekoop, and A. Venema, "Love waves for (bio)-chemical sensing in liquids," in *Proc. IEEE Ultrasonics Symp.*, 1992, pp. 281–285.

[9] E. Gizeli, "Design considerations for the acoustic waveguide biosensor," *Smart Mater. Struct.*, vol. 6, no. 6, 1997 , Art. no. 700.

[10] C.-T. Feng, C.-J. Cheng, and M. Z. Atashbar, "PMMA/64° YX-LiNbO 3 guided SH-SAW based immunosensing system," *IEEE SENSORS*, vol. 2011, pp. 308–311, 2011, doi: 10.1109/ICSENS.2011.6127240.

[11] P. Roach, S. Atherton, N. Doy, G. McHale, and M. I. Newton, "SU-8 guiding layer for love wave devices," *Sensors*, vol. 7, no. 11, pp. 2539–2547, 2007.

[12] C. McMullan, H. Mehta, E. Gizeli, and C. R. Lowe, "Modelling of the mass sensitivity of the love wave device in the presence of a viscous liquid," *J. Phys. D: Appl. Phys.*, vol. 33, no. 23, 2000, Art. no. 3053.

[13] G. Xu, "Direct finite-element analysis of the frequency response of a YZ lithium niobate SAW filter," *Smart Mater. Struct.*, vol. 9, no. 6, p. 973, 2000.

[14] K. M. Kabir, G. I. Matthews, Y. M. Sabri, S. P. Russo, S. J. Ippolito, and S. K. Bhargava, "Development and experimental verification of a finite element method for accurate analysis of a surface acoustic wave device," *Smart Mater. Struct.*, vol. 25, no. 3, 2016, Art. no. 035040.

[15] M. M. El Gowini and W. A. Moussa, "A finite element model of a MEMS-based surface acoustic wave hydrogen sensor," *Sensors*, vol. 10, no. 2, pp. 1232–1250, 2010.

[16] S. Lee, K. B. Kim, and Y. I. Kim, "Mass sensitivity calculation of the protein layer using love wave SAW biosensor," *J. Nanosci. Nanotechnol.*, vol. 12, no. 7, pp. 6107–6112, 2012.

[17] X.-C. Lo, J.-Y. Li, M.-T. Lee, and D.-J. Yao, "Frequency shift of a SH-SAW biosensor with glutaraldehyde and 3-Aminopropyltriethoxysilane functionalized films for detection of epidermal growth factor," *Biosensors*, vol. 10, no. 8, 2020 , Art. no. 92.

[18] B. D. Grant, C. A. Smith, K. Karvonen, and R. Richards-Kortum, "Highly sensitive two-dimensional paper network incorporating biotin–streptavidin for the detection of malaria," *Anal. Chem.*, vol. 88, no. 5, pp. 2553–2557, 2016.

[19] P. Tiwary, "Molecular determinants and bottlenecks in the dissociation dynamics of biotin–streptavidin," *J. Phys. Chem. B*, vol. 121, no. 48, pp. 10841–10849, 2017.

[20] S. Maiti and P. Paira, "Biotin conjugated organic molecules and proteins for cancer therapy: A review," *Eur. J. Med. Chem.*, vol. 145, pp. 206–223, 2018, doi: 10.1016/j.ejmech.2018.01.001.

[21] P. Aisen, "Transferrin receptor 1," *Int. J. Biochem. Cell Biol.*, vol. 36, no. 11, pp. 2137–2143, 2004.

[22] H. O. Habashy *et al.*, "Transferrin receptor (CD71) is a marker of poor prognosis in breast cancer and can predict response to tamoxifen," *Breast Cancer Res. Treat.*, vol. 119, no. 2, 2010, Art. no. 283.

[23] G. Magro *et al.*, "Aberrant expression of tfr1/CD71 in thyroid carcinomas identifies a novel potential diagnostic marker and therapeutic target," *Thyroid*, vol. 21, no. 3, pp. 267–277, 2011.

[24] M. Ohkuma *et al.*, "Absence of CD71 transferrin receptor characterizes human gastric adenosquamous carcinoma stem cells," *Ann. Surg. Oncol.*, vol. 19, no. 4, pp. 1357–1364, 2012.

[25] Y. Kohgo, T. Nishisato, H. Kondo, N. Tsushima, Y. Niitsu, and I. Urushizaki, "Circulating transferrin receptor in human serum," *Brit. J. Haematol.*, vol. 64, no. 2, pp. 277–281, 1986.

[26] A. Åkesson, P. Bjellerup, and M. Vahter, "Evaluation of kits for measurement of the soluble transferrin receptor," *Scand. J. Clin. Lab. Investigation*, vol. 59, no. 2, pp. 77–81, 1999.

[27] A. Hikawa, Y. Nomata, T. Suzuki, H. Ozasa, and O. Yamada, "Soluble transferrin receptor-transferrin complex in serum: Measurement by latex agglutination nephelometric immunoassay," *Clin. Chimica Acta*, vol. 254, no. 2, pp. 159–172, 1996.

[28] S. Trivedi and H. B. Nemade, "Finite element simulation of a highly sensitive SH-SAW delay line sensor with SiO_2 micro-ridges," *Microsyst. Technol.*, vol. 24, no. 8, pp. 3537–3547, 2018.

[29] S. Trivedi and H. B. Nemade, "Coupled resonance in SH-SAW resonator with S1813 micro-ridges for high mass sensitivity biosensing applications," *Sensors Actuators B: Chem.*, vol. 273, pp. 288–297, 2018, doi: org/10.1016/j.snb.2018.06.040.

[30] K. Han and Y. J. Yuan, "Mass sensitivity evaluation and device design of a love wave device for bond rupture biosensors using the finite element method," *IEEE Sensors J.*, vol. 14, no. 8, pp. 2601–2608, Aug. 2014.
[31] G. Zhang, "Nanostructure-enhanced surface acoustic waves biosensor and its computational modeling," *J. Sensors*, vol. 2009, 2009.
[32] Y. Li and O. Bou Matar, "Convolutional perfectly matched layer for elastic second-order wave equation," *J. Acoust. Soc. Am.*, vol. 127, no. 3, pp. 1318–1327, 2010.
[33] R. Manenti, *Surface Acoustic Wave Resonators for Quantum Information*. Citeseer, 2013.
[34] Q. Zhang, C. Xue, Y. Yuan, J. Lee, D. Sun, and J. Xiong, "Fiber surface modification technology for fiber-optic localized surface plasmon resonance biosensors," *Sensors*, vol. 12, no. 3, pp. 2729–2741, 2012.
[35] B. Tao and C. Xian-Hua, "Preparation and characterization of lanthanum-based thin films on sulfonated self-assembled monolayer of 3-mercaptopropyl trimethoxysilane," *Thin Solid Films*, vol. 515, no. 4, pp. 2262–2267, 2006.
[36] R. A. Vijayendran and D. E. Leckband, "A quantitative assessment of heterogeneity for surface-immobilized proteins," *Anal. Chem.*, vol. 73, no. 3, pp. 471–480, 2001.
[37] J. Zhu, T. Nguyen, R. Pei, M. Stojanovic, and Q. Lin, "Specific cell capture and temperature-mediated release using surface-immobilized aptamers in a microfluidic device," in *Proc. IEEE 16th Int. Solid-State Sensors, Actuators Microsyst. Conf.*, 2011, pp. 751–754.
[38] Z. Li, Y. Jones, J. Hossenlopp, R. Cernosek, and F. Josse, "Design considerations for high sensitivity guided SH-SAW chemical sensor for detection in aqueous environments," in *Proc. IEEE Int. Freq. Control Symp. Expo.*, 2004, pp. 185–192.
[39] F. Josse, F. Bender, R. Cernosek, and K. Zinszer, "Guided SH-SAW sensors for liquid-phase detection," in *Proc. IEEE Int. Frequncy Control Symp. PDA Exhib.*, 2001, pp. 454–461.
[40] A. A. Kortt, E. Nice, and L. C. Gruen, "Analysis of the binding of the fab fragment of monoclonal antibody NC10 to influenza virus N9 neuraminidase from tern and whale using the BIAcore biosensor: Effect of immobilization level and flow rate on kinetic analysis," *Anal. Biochem.*, vol. 273, no. 1, pp. 133–141, 1999.

XUE-CHANG LO received the M.S. degree from the Department of Engineering and System Science, National Tsing Hua University, Taiwan, in 2020. After graduation, he joined TSMC as an Engineer. His research interests include MEMS, bioengineering, and microfluidics.

MING-TSANG LEE received the Ph.D. degree from the Department of Mechanical Engineering, University of California at Berkeley in 2008. He is an Associate Professor with the Department of Power Mechanical Engineering, National Tsing Hua University, Taiwan. His research interests include sustainable energy systems, wearable electronics, opto-thermal-fluidic coupled transport phenomena, and micro/nanoscale heat transfer.

DA-JENG YAO (Senior Member, IEEE) received the M.S. degree from the Department of Mechanical Engineering, Lehigh University in 1996, and the Ph.D. degree from the Department of Mechanical and Aerospace Engineering, UCLA in 2001. He is a Professor with the Institute of Nano Engineering and Micro Systems (NEMS), National Tsing Hua University, Taiwan. His research interests include fertilization on a chip, intelligent gas sensing system and its applications, digital microfluidic systems, and THz applications.